# Effect of bath ionic strength on adhesion and tribological properties of pure nickel and nickel composite coatings

Rizwan Bajwa[1], Zulfiqar Khan[1], Vasilios Bakolas[2], Wolfgang Braun[2]

[1]*Sustainable Design Research Centre, Faculty of Science & Technology, Bournemouth University Talbot Campus, Poole, Dorset, United Kingdom*

[2]*Advanced Bearing Analysis, Schaeffler Technologies GmbH & Co. KG, 91074 Herzogenaurach, Germany*

[1]Email: rbajwa@bournemouth.ac.uk

**Abstract**

The effect of electrolytic chemical concentration on wear-resistance, corrosion-resistance, adhesion and wettability properties of pure nickel and nickel-alumina composite coatings has been investigated in this paper. Coatings were electroplated over steel substrates under constant pulse conditions using pulse electrodeposition technique. Corrosion-resistance results show that the anti-corrosion properties are increasing with medium concentration both for pure nickel and nickel-alumina composite coating. For anti-wear properties the medium concentration showed increasing trend in case of pure nickel coatings but decreased in nickel-alumina composite coatings. In composite coating the higher and low concentrations of electrolyte showed the higher wear resistance properties. Furthermore, the influence of electrolyte concentration on changing surface morphologies, mechanical, wettability and adhesion properties have been investigated and reported here. Surface morphologies of the synthesized coatings were studied with scanning electron microscopy and energy-dispersive spectroscopy. Coatings surface mapping and wear analyses were examined by using 3D white light interferometry.

***Keywords:*** *wear-resistance, corrosion resistance, adhesion, water-lubrication*

## 1. Introduction

Electrodeposited composite coatings incorporating hard nanoparticle oxides as $Al_2O_3$ [1, 2], ZrO [3, 4], TiO [5], $Fe_2O_3$ [6],$CeO_2$ [7] and carbides as SiC [8, 9] or WC [10] demonstrated excellent tribological and mechanical properties with wide ranging industrial applications in engineering.

The electrodeposition techniques provide a freedom of controlling a variety of coating parameters with enhanced mechanical and tribological properties. This freedom allows significant contribution for the design of nanocomposite coatings in terms of surface engineering. Due to wide range of experimental parameters in pulse electrodeposition technique many experimental results presented in the literature are contradictory or difficult to compare [11, 12, 13]. There are two main types of electrodeposition conditions 1): pulse parameters which include current density, pulse-on time/pulse-off time, duty cycle and frequency and 2): bath conditions; these include bath composition, additives, pH, temperature and composite micro/nano sized particles. Extensive studies have been conducted with improved mechanical and tribological properties of electrodeposited coatings by properly controlling these parameters [14, 15, 16, 17, 18, 19]. However, the effect of ionic strength of electrolyte solution on wear-resistance and corrosion-resistance properties left obscure and needs to be explore due to their utmost important in wide range of industrial applications as a wear and corrosion resistance protective coatings.

This work is the continuation of research within our group [20, 21, 22, 23, 24]. The purpose of this investigation is to demonstrate an optimised bath concentration for electrodeposited coatings in terms of improved tribological and mechanical properties for water-lubricated tribological systems/components. Previously, Lehman and co-workers have conducted experimental investigations to understand the influence of electrolyte composition on the electrodeposited coatings [25]. They presented that lower ionic concentration contribute to better deposition with respect to microstructure and better dispersion of particles in matrix of pure nickel and Ni-$Al_2O_3$ composite coatings. The effect of bath volume for electrodeposition was explored by Daniel and co-workers [26]. Their findings were that the high volume of bath solution progressively increased the deposition rate of nickel coating through electrodeposition process. They investigated the microstructure and mechanical properties analysis of the coatings without tribological performance measures.

During the current work electrolytes were prepared with three varying strengths (high, medium and low concentrations) in total six baths (every two baths with same strength) for electrodeposition of Ni-$Al_2O_3$ composite and pure nickel coatings.

The tribological properties of these coatings investigated using High Speed Microprocessor Rotary Tribometer (HSMRT) to simulate industrial applications in terms of rolling contacts. Pure nickel coatings were manufactured as a reference coating and investigated under the same chemical and tribo test conditions.

## 2. Experimental methods

### *2.1. Preparation and characterization of coatings*

All coatings, the pure nickel and the composites incorporating nano-$Al_2O_3$, were deposited under constant pulse parameters as; current density 3A/$dm^2$, pulse on/off time 20/80ms respectively and with a duty cycle of 20% with expected thickness of ~10µm.

The Watt's-type bath prepared with different ionic strength of bath solution as high concentration (HC), medium concentration (MC) and low concentration (LC) for both pure nickel and composite coatings. 20 g/L of nano-alumina (~50nm) supplied by Io-Li-Tec (Germany), was added to bath for developing composite coatings. The solutions had been magnetically stirred overnight to yield better suspension prior to the start of the deposition process. In addition these nanoparticles were ultrasonically dispersed in the electrolyte during the deposition process. The composition of chemical within the bath included nickel sulphate, nickel chloride, boric acid and nanoparticles which are provided in Table 1.

Nickel sheet (99.99% purity) was used as anode and a steel substrate (80mm diameter and 8.20mm thick) was used as a cathode. The chemical composition of steel substrate is given in Table 2. The substrate disc with a surface area (0.70 $dm^2$) to be deposited was mechanically polished to achieve naked substrate constant roughness (Ra) of 0.05µm for all samples. The surface area which was not required to be electroplated was sealed with polyvinyl chloride PVC. Prior to each coating deposition the substrate surface conditioning performed using deionized water and acetone under ultrasonic treatment. The pH of the bath was adjusted between 4.0-4.5 by sodium hydroxide or diluted sulphuric acid and recorded using Tecpel pH meter. The surface roughness measurements were performed by using three-dimensional scanning interferometry (ZYGO). The roughness parameters Ra and Rz, defined as the arithmetic mean of roughness profile and sum of maximum values of profile peak height and depth respectively over the entire sampling length.

Scanning Electron Microscopy (JSM-6010, JEOL) was used to analyse the surface morphology of the coatings. For cross-section view of coating-substrate interface adhesion the samples were imbedded by ATM OPAL 460 equipment keeping coatings cross-sectional areas on top. Mechanical properties including hardness and elastic modulus of coatings were calculated by using CSM Micro Indentation Tester (MHT) at a loading force of 300mN. At least 12 indentations were made on each sample and average value is report with error bars.

### 2.2. *Tribological and anti-corrosion properties testing*

The wear resistance tests conducted using a ball-on-plate machine assembled to a High Speed Microprocessor Rotary Tribometer (HSMRT) and described in [27]. The unidirectional ball-on-disc tribometer consists of upper coated disc and lower three steel balls (100Cr6) equally spaced at 120°. Previously, such ball-on-plate rig have been used to study rolling contact fatigue response when ball is in rolling contact with a flat surface [28, 29]. The hardness and elastic modulus of ball was 740+140 HV10 and 210 GPa, respectively. All tests performed in distilled water at a rolling speed of 1 m/s and normal load of 45N under boundary/mixed lubrication regimes condition. The corresponding Hertzian contact pressure [30] can be estimated to 1.75 GPa, assuming contact between steel ball (210GPa, Poisson's ratio 0.30) and coated flat disc (230GPa, Poisson's ratio 0.28 [31]).

The cross-sectional area of worn surface was measured by using a three-dimensional surface profiler (ZYGO) to calculate the amount of wear of the coating. The wear volume is defined as V=AL, where A is the cross-sectional area of wear track ($mm^2$) and L is the length of the wear track (mm). A specific wear rate was determined as: Specific wear rate ($mm^3$/Nm) = Wear volume ($mm^3$)/[Load (N) x rolling distance (m)] [32]. To ensure repeatability and to minimize uncertainty each test was perform at least two times under the same testing conditions.

The potentiodynamic anodic polarization measurements were carried out using three-electrode system with a platinum wire as counter electrode and Ag+/AgCl electrode as reference electrode. The coated samples were used as working electrode. The coated specimens were immersed in 3.5 wt. % NaCl electrolyte at a temperature of 20C° till the OCP was stable before staring the test at scanning rate 0.001 V/s. The corrosion resistance properties of the coatings were studied from potentiodynamic anodic polarization curves.

### 2.3. *Adhesion and wettability testing*

The scratch testing method was used to study the adhesion of coating according to DIN EN 1071-3 standard method (Determination of adhesion and other mechanical failure modes by a scratch test). The scratch tests were conducted using a CSM REVETEST machine with Rockwell C diamond with a tip radius of 200µm. The scratch length of 10 mm was made with sliding speed of 10mm/min. The load was increased from 0 N to 100 N/min. The smallest load at which first failure mode was observed defined critical load value.

The wettability behaviour of coatings studied using Owens and Wendt (OWRK) method [33]. To ensure the statistical validity of the results, two to three droplets were made for contact angle measurements using water and diiodomethane as reference liquids of known surface energies. The determination of the surface energies of the solid coatings based on contact angle measurements methodology is explained in detail elsewhere [34].

## 3. Results and discussion

### *3.1. Surface morphology and mechanical properties*

Fig. 1 compares the engineered surfaces through SEM micrographs of which were produced by using various bath concentrations (HC, MC and LC). As can be seen from Figure 1, in case of HC and MC the surface morphologies of nickel and nickel composite coatings were not affected with deposition from different concentration of ionic strength of electrolyte. Whilst, for coatings deposited from LC concentration resulted into bigger grain structure and agglomeration clusters in pure nickel and Ni-alumina composite coatings respectively. This change in morphology subject to lower concentration of bath was also evident from surface roughness parameters (Ra and Rz), shown in Fig. 2. Due to the presence of agglomerated particles in Ni-$Al_2O_3$ (LC) composite exhibits the maximum surface roughness (Ra~0.64µm; Rz~4.36µm), followed by pure nickel (LC) coatings with Ra~0.08µm and Rz~0.98µm values because of bigger grain structure. Agglomerated particles on the surface resulted in larger standard deviation value of roughness parameters of Ni-$Al_2O_3$ (LC) composite coating. It was interesting to note that similar behaviour was observed in microhardness results of these coatings with variation in ionic strength of electrolyte. Likewise, there were not significant differences in measured hardness (350-450HV), deposited from HC and MC strength for both pure and composite coatings except the LC type coatings (Fig. 3). The reason for the highest hardness for pure Ni (MC) when compared to pure Ni (HC) and pure Ni (LC) can be attributed to relatively much finer, more compact and smaller grain size morphology as shown in Figure 1 (a-c). The microhardness of Ni-$Al_2O_3$ (LC) was significantly improved in LC bath with average value of 515HV as compared to pure nickel deposited from LC bath with average value of 230HV. The maximum value of hardness in Ni-alumina composite deposited LC type bath predicts better anti-wear performance of these coatings. However, the higher surface roughness parameters of these type of coatings can attribute to surface friction which can be reduced through surface polishing prior to real applications. Note that the samples were mechanically polished to

achieve relative smoother surface prior to mechanical testing. This is because that the roughness peak coming in contact to indenter can result in a greater depth of indent at relatively lower load due to increased localized stress at the point of contact.

In comparison, the typical pyramidal and spherical globular shape microstructure morphologies observed in pure nickel and nickel-based composite coatings respectively. Similar morphologies in nickel and nickel based composite have been reported previously by different researchers [35, 36, 37, 38]. Moreover addition of alumina nanoparticles in nickel matrix resulted into the compact morphology as compared to pure nickel coatings. This attributed to well-known cathodic polarization phenomenon due to the adsorption of particles at substrate surface. All pure nickel and nickel-based coatings were smooth, crack free and well adhere to the substrate without an interfacial delamination as shown in Figure 4 (a-f). To see the effect of electrolyte concentration on nano-alumina particles distribution in composite coatings magnified view of cross-sectional images is presented in Figure 4(d-f). All composite coatings exhibit the homogenous nano-alumina particles distribution. However, less agglomerated nano-$Al_2O_3$ particles were observed in LC type coatings than those produced by HC and MC type electrolyte. In addition to homogenous particle distribution the less agglomeration behaviour can be the reason for the higher hardness value of Ni-$Al_2O_3$ (LC) coating.

### *3.2. Tribological and wettability properties*

Generally, the wear-resistance properties of electroplated coatings improved with addition of hard nanoparticles into matrix materials as can be seen from Fig. 5. This is attributed to the strengthening effects of loaded hard particles into nickel matrix and in agreement with previous findings [3, 39, 40]. The influence of reagent concentration on pure nickel coatings demonstrated that the MC type coating has less wear about 30% than HC and about half of LC type coatings. A reason for this can be the higher hardness of MC as compared to HC and LC type's coatings. Also, the higher plasticity index H/E ratio of pure Ni (MC) than those pure Ni (HC) and pure Ni (LC) can result in better wear resistance properties [41]. A comparison between composite coatings showed that HC and LC type composites exhibit the similar wear-resistance behaviour and almost half of the composite coating deposited from MC electrolyte. When compared with pure nickel coatings the wear resistance of composite coating is improved, almost doubled, except MC type which enhanced about 25% of the MC type pure nickel coating. Also, mean-steady friction

coefficient values are lower for composite coatings than that of pure nickel coatings, as can be seen in Figure 5. The strengthening effect of incorporated nano-alumina particle is the reason for the lower friction coefficient of composite coatings. It is known that the friction coefficient in composite coatings was reduced with increasing the reinforcement content of nanoparticles in the coatings [3, 42]. The higher wear rate in MC type composite coating may be due to the lower surface wettability behaviour, resulting into dry contact wear scenario. The effect of changing bath concentration on coatings surface wettability behaviour plotted in Fig. 6. In all coatings the higher dispersive part than polar part of surface free energy reveals that coatings exhibit mainly covalent bonds. However, MC type nickel alumina composite showed the minimum value of polar component, consequently the maximum contact angle of water was observed. This can be the one reason for higher wear rate than other composite coatings due to decreased wettability. These results indicate that in order to achieve better anti-wear properties MC composition is suitable in pure nickel coatings. On the other hand, HC and LC electrolytes can produce better wear resistance properties in nickel based composite coatings reinforced with nano-alumina particles.

### *3.3. Electrochemical corrosion-resistance properties*

To evaluate the optimized bath concentration for pure nickel and nickel composite coatings the electrochemical corrosion measurements deployed and resulting potentiodynamic polarization curves are plotted in Fig. 7. As can be seen from Fig. 7 under the same conditions the composite coatings showed better anti-corrosion property than pure nickel coatings and validates the previous finding in the literature [43]. It is interesting to observe that the coatings deposited from MC type electrolyte exhibits the maximum corrosion resistance potential both in pure nickel and nickel based nano-alumina composites. Note that in pure nickel coatings deposited from MC bath also performed better in term of wear resistance. Therefore medium concentration is suitable solution to get better wear and corrosion resistance properties for pure nickel coatings. For Ni-$Al_2O_3$ composite coatings the MC better candidate to corrosion resistance but not suitable for wear resistance in comparison to HC and LC solutions. However, the corrosion performance of LC type composite coatings can be improved by surface polishing to reduce surface roughness which can be the main reason for poor corrosion resistance behaviour. This is well-known that the roughness valleys in the surface can provide weak point for the penetration of aggressive corrosive solution towards substrate and can result into poor corrosion resistance performance.

### *3.4. Adhesion strength properties*

The coating-substrate interface adhesion strength is one of the important factors of the coating in industrial applications. Therefore adhesion strength was evaluated through scratch test for these coatings and compared with minimum critical load value required in industrial applications. The effects of different bath conditions on adhesion critical load values (Lc) for electrodeposited coatings are compared and presented in Fig. 8. As can be seen all the coatings showed good adhesion strength except in case of pure nickel deposited from HC electrolyte. In pure nickel coatings the maximum critical load value of 44N observed in MC type bath and followed by LC and HC with values 50N and 44N respectively. For nickel composite coatings, the critical load values ranges between 60 to 80N which is significantly higher than pure nickel coatings. Note that these coatings were deposited on mild steel substrate without any intermediate coating which can further improve adhesion strength.

## 4. Conclusions

Tribological and adhesion properties of electrodeposited pure nickel and nickel composite coatings with incorporated nano-alumina particles coatings have been studied. The effects of different ionic strength of electrolyte on these properties investigated to evaluate optimized concentration of bath. The following conclusions can be drawn from experimental results.

- In general the influence of bath concentration on surface morphology and mechanical properties of all coatings was much significant. However, MC and LC type baths showed better hardness values in pure nickel and nickel-alumina composites respectively.
- Wear-resistance properties increase with HC and LC type bath in nickel-alumina composite coatings. Whereas, wear-resistance properties decreased in HC and LC type and increased in MC type bath.
- The electrochemical corrosion results show that the MC type bath is suitable candidate to achieve increased corrosion resistance properties both in pure nickel and nickel composite coatings.
- The scratch tests show that independent from bath type, the adhesion significantly increase with incorporation of nanoparticles into nickel matrix. The minimum adhesion strength observed in LC type pure nickel coatings.

## ACKNOWLEDGEMENTS

This work was performed with financial and in-kind support from Schaeffler Technologies GmbH & Co. KG (Germany) and Bournemouth University (UK) as part of a collaborative research programme.

## REFERENCE

1. Lee C. Wear and corrosion behavior of electrodeposited nickel–carbon nanotube composite coatings on Ti–6Al–4V alloy in Hanks′ solution. Tribology International. 2012;55:7-14.

2. Lee C. Corrosive Wear and Mechanical Properties of Ni/Al2O3 Micro-and Nanoparticulates-Reinforced Coatings on Ti-6Al-4V Alloy. Tribology Transactions. 2012;55:640-51.

3. Borkar T, Harimkar SP. Effect of electrodeposition conditions and reinforcement content on microstructure and tribological properties of nickel composite coatings. Surface and Coatings Technology. 2011;205:4124-34.

4. Dass K, Chauhan S, Gaur B. Study on Mechanical and Dry Sliding Wear Characteristics of Meta-Cresol Novalac Epoxy Composites Filled with Silicon Carbide, Aluminum Oxide, and Zinc Oxide Particulates. Tribology Transactions. 2014;57:157-72.

5. Lajevardi S, Shahrabi T. Effects of pulse electrodeposition parameters on the properties of Ni–TiO< sub> 2</sub> nanocomposite coatings. Applied Surface Science. 2010;256:6775-81.

6. Haq IU, Akhtar K, Khan TI, Ali Shah A. Electrodeposition of Ni–Fe< sub> 2</sub> O< sub> 3</sub> nanocomposite coating on steel. Surface and Coatings Technology. 2013;235:691-8.

7. Xue Y-J, Liu H-B, Lan M-M, Li J-S, Li H. Effect of different electrodeposition methods on oxidation resistance of Ni–CeO< sub> 2</sub> nanocomposite coating. Surface and Coatings Technology. 2010;204:3539-45.

8. Rudnik E, Burzyńska L, Dolasiński Ł, Misiak M. Electrodeposition of nickel/SiC composites in the presence of cetyltrimethylammonium bromide. Applied Surface Science. 2010;256:7414-20.

9. Pradhan AK, Das S. Dry Sliding Wear and Friction Behavior of Cu-SiC Nanocomposite Coating Prepared by Pulse Reverse Electrodeposition. Tribology Transactions. 2014;57:46-56.

10. Surender M, Basu B, Balasubramaniam R. Wear characterization of electrodeposited Ni–WC composite coatings. Tribology International. 2004;37:743-9.

11. Hovestad A, Janssen L. Electrochemical codeposition of inert particles in a metallic matrix. Journal of Applied Electrochemistry. 1995;25:519-27.

12. Gomes A, Pereira I, Fernández B, Pereiro R. Electrodeposition of metal matrix nanocomposites: improvement of the chemical characterization techniques. Advances in Nanocomposites-Synthesis, Characterization and Industrial Applications, Boreddy Reddy (Ed), InTech. 2011:503.

13. Golchin A, Simmons G, Glavatskih S, Prakash B. Tribological behaviour of polymeric materials in water-lubricated contacts. Proceedings of the Institution of Mechanical Engineers, Part J: Journal of Engineering Tribology. 2013:1350650113476441.

14. Low C, Wills R, Walsh F. Electrodeposition of composite coatings containing nanoparticles in a metal deposit. Surface and Coatings Technology. 2006;201:371-83.

15. Chandrasekar M, Pushpavanam M. Pulse and pulse reverse plating—Conceptual, advantages and applications. Electrochimica Acta. 2008;53:3313-22.

16. Scharf T, Prasad S. Solid lubricants: a review. Journal of materials science. 2013;48:511-31.

17. Balasubramanian A, Srikumar D, Raja G, Saravanan G, Mohan S. Effect of pulse parameter on pulsed electrodeposition of copper on stainless steel. Surface Engineering. 2009;25:389-92.

18. Rashidi A, Amadeh A. Effect of electroplating parameters on microstructure of nanocrystalline nickel coatings. Journal of Materials Science & Technology. 2010;26:82-6.

19. Xuetao Y, Yu W, Dongbai S, Hongying Y. Influence of pulse parameters on the microstructure and microhardness of nickel electrodeposits. Surface and Coatings Technology. 2008;202:1895-903.

20. Nazir M, Khan ZA, Stokes K. Optimisation of interface roughness and coating thickness to maximise coating–substrate adhesion–a failure prediction and reliability assessment modelling. Journal of Adhesion Science and Technology. 2015;29:1415-45.

21. Khan ZA, Pashaei P, Bajwa R, Nazir H, Cakmak M. Fabrication and characterisation of electropdeposited and magnertron-sputtered thin films. International Journal of Computational Methods & Experimental Measurements. 2015:1-10.

22. Nazir M, Khan ZA, Stokes K. A holistic mathematical modelling and simulation for cathodic delamination mechanism–a novel and an efficient approach. Journal of Adhesion Science and Technology. 2015:1-39.

23. Nazir M, Khan ZA, Stokes K. A unified mathematical modelling and simulation for cathodic blistering mechanism incorporating diffusion and fracture mechanics concepts. Journal of Adhesion Science and Technology. 2015;29:1200-28.

24. Nazir M, Khan Z, Stokes K. Modelling of metal-coating delamination incorporating variable environmental parameters. Journal of Adhesion Science and Technology. 2015;29:392-423.

25. Bełtowska-Lehman E, Goral A, Indyka P. Electrodeposition and characterization of Ni/Al2O3 nanocomposite coatings. Archives of Metallurgy and Materials. 2011;56:919-31.

26. Oloruntoba D, Eghwubare O, Oluwole O. Effect of Some Process Variables on Nickel Electroplating of Low Carbon Steel. Leonardo Electronic Journal of Practices and Technologies. 2010.

27. Khan ZA, Hadfield M, Wang Y. Pressurised chamber design for conducting rolling contact experiments with liquid refrigerant lubrication. Materials & design. 2005;26:680-9.

28. Kikuchi K, Yoshioka T, Kitahara T, Ozaki K, Nakayama K, Fujiwara T. Rolling contact fatigue life of ceramics for rolling bearing materials. Japan Society of Lubrication Engineers, Journal-International Edition,(ISSN 0389-5483). 1984:137-42.

29. FUJIWARA T, YOSHIOKA T, KITAHARA T, KOIZUMI S, TAKEBAYASHI H. Study on load rating property of silicon nitride for rolling bearing material. Japan Society of Lubrication Engineers, Journal-International Edition. 1989:81-6.

30. Johnson K. Contact mechanics. 1985. Cam-bridge University Press, Cambridge. 1974.

31. Lille H, Koo J. Determination of the Modulus of Elasticity, Poisson's Ratio and the Coefficient of Thermal Expansion of Electrochemically Metallized Nickel Coatings. Materials Science. 2005;11:356-9.

32. Cui G, Bi Q, Zhu S, Fu L, Yang J, Qiao Z, Liu W. Synergistic effect of alumina and graphite on bronze matrix composites: Tribological behaviors in sea water. Wear. 2013;303:216-24.

33. Owens DK, Wendt R. Estimation of the surface free energy of polymers. Journal of applied polymer science. 1969;13:1741-7.

34. Lugscheider E, Bobzin K. The influence on surface free energy of PVD-coatings. Surface and Coatings Technology. 2001;142:755-60.

35. Jegan A, Venkatesan R. Characterization and optimization of pulse electrodeposition of Ni/nano-Al2O3 composite coatings. International Journal of Minerals, Metallurgy, and Materials. 2013;20:479-85.

36. Jung A, Natter H, Hempelmann R, Lach E. Nanocrystalline alumina dispersed in nanocrystalline nickel: enhanced mechanical properties. Journal of materials science. 2009;44:2725-35.

37. Thiemig D, Lange R, Bund A. Influence of pulse plating parameters on the electrocodeposition of matrix metal nanocomposites. Electrochimica Acta. 2007;52:7362-71.

38. Thiemig D, Bund A. Influence of ethanol on the electrocodeposition of Ni/Al2O3 nanocomposite films. Applied Surface Science. 2009;255:4164-70.

39. Wang S-C, Wei W-CJ. Characterization of electroplated Ni/SiC and Ni/Al 2 O 3 composite coatings bearing nanoparticles. Journal of materials research. 2003;18:1566-74.

40. Wielage B, Lampke T, Zacher M, Dietrich D, Electroplated nickel composites with micron-to nano-sized particles. 2008: Publisher.

41. Wang Q, Zhou F, Ding X, Zhou Z, Wang C, Zhang W, Li LK-Y, Lee S-T. Microstructure and water-lubricated friction and wear properties of CrN (C) coatings with different carbon contents. Applied Surface Science. 2013;268:579-87.

42. Fan H, Electroplating of Compound Ni–SiC Coatings and Improvement of Wear Resistance. 2010: Publisher.

43. Feng Q, Li T, Teng H, Zhang X, Zhang Y, Liu C, Jin J. Investigation on the corrosion and oxidation resistance of Ni–Al 2 O 3 nano-composite coatings prepared by sediment co-deposition. Surface and Coatings Technology. 2008;202:4137-44.

Table

**Table 1 Chemical and nanoparticles composition for varying bath concentration.**

| Bath number | Chemical composition (g/L) | | | |
|---|---|---|---|---|
| | Nickel sulfate | Nickel chloride | Boric acid | Nano-$Al_2O_3$ |
| | **High concentration (HC)** | | | |
| 1 | 331 | 60 | 38 | - |
| 2 | 331 | 60 | 38 | 20 |
| | **Medium concentration (MC)** | | | |
| 3 | 265 | 48 | 31 | - |
| 4 | 265 | 48 | 31 | 20 |
| | **Low concentration (LC)** | | | |
| 5 | 200 | 48 | 31 | - |
| 6 | 200 | 48 | 31 | 20 |

**Table 2 Chemical composition of the steel substrate**

| C (wt.%) | Si (wt.%) | Mn (wt.%) | S (wt.%) | P (wt.%) |
|---|---|---|---|---|
| 0.14 | 0.27 | 0.91 | 0.25 | 0.02 |

Figure1 Surface micrographs of pure nickel (a-c) and Ni-Al2O3 composite (e-g) coatings deposited through various bath compositions (1

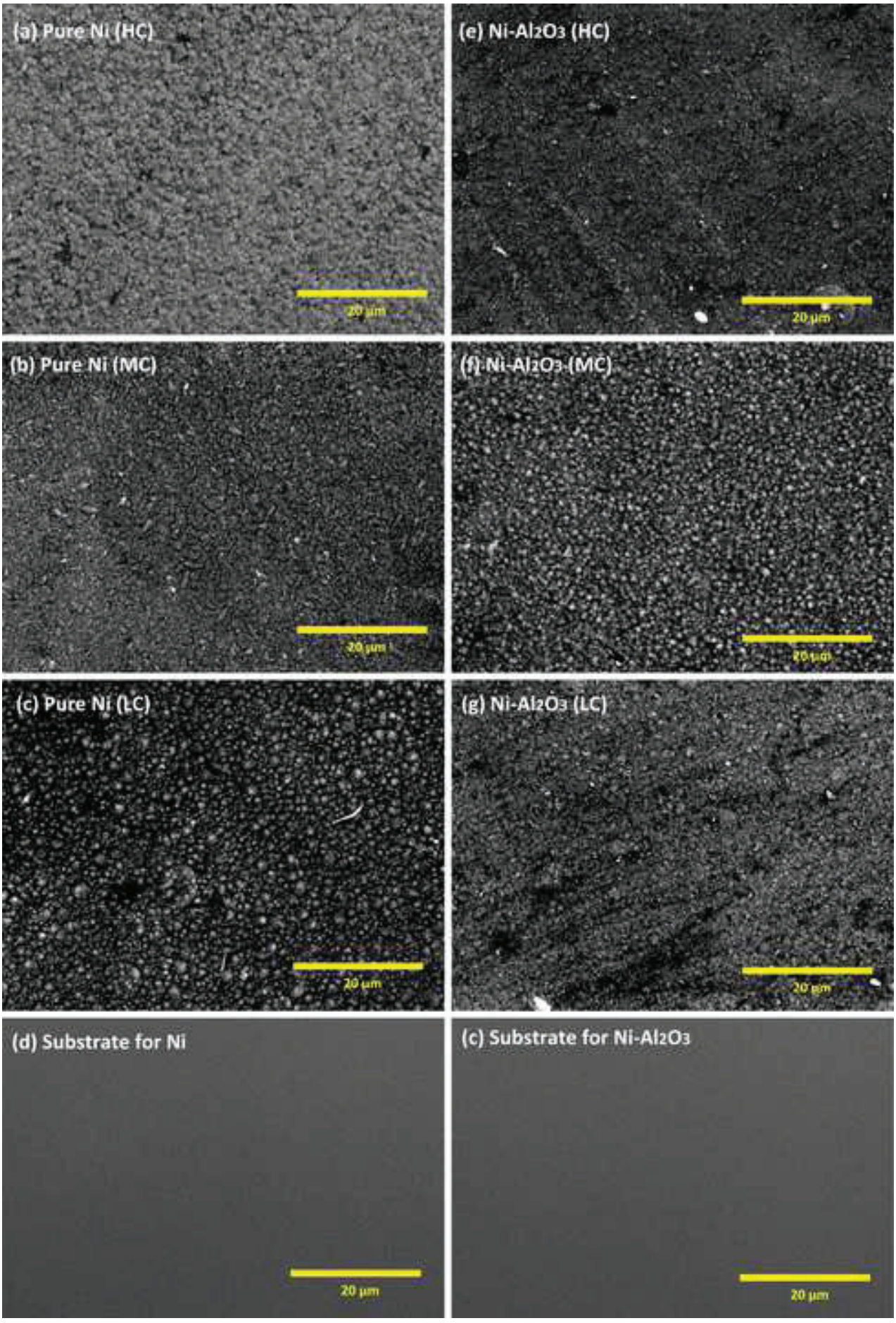

Figure2 The variation in surface roughness parameters (Ra and Rz) of electrodeposited coatings with different electrolyte ionic strength. Click here to download Figure Figure2.tif

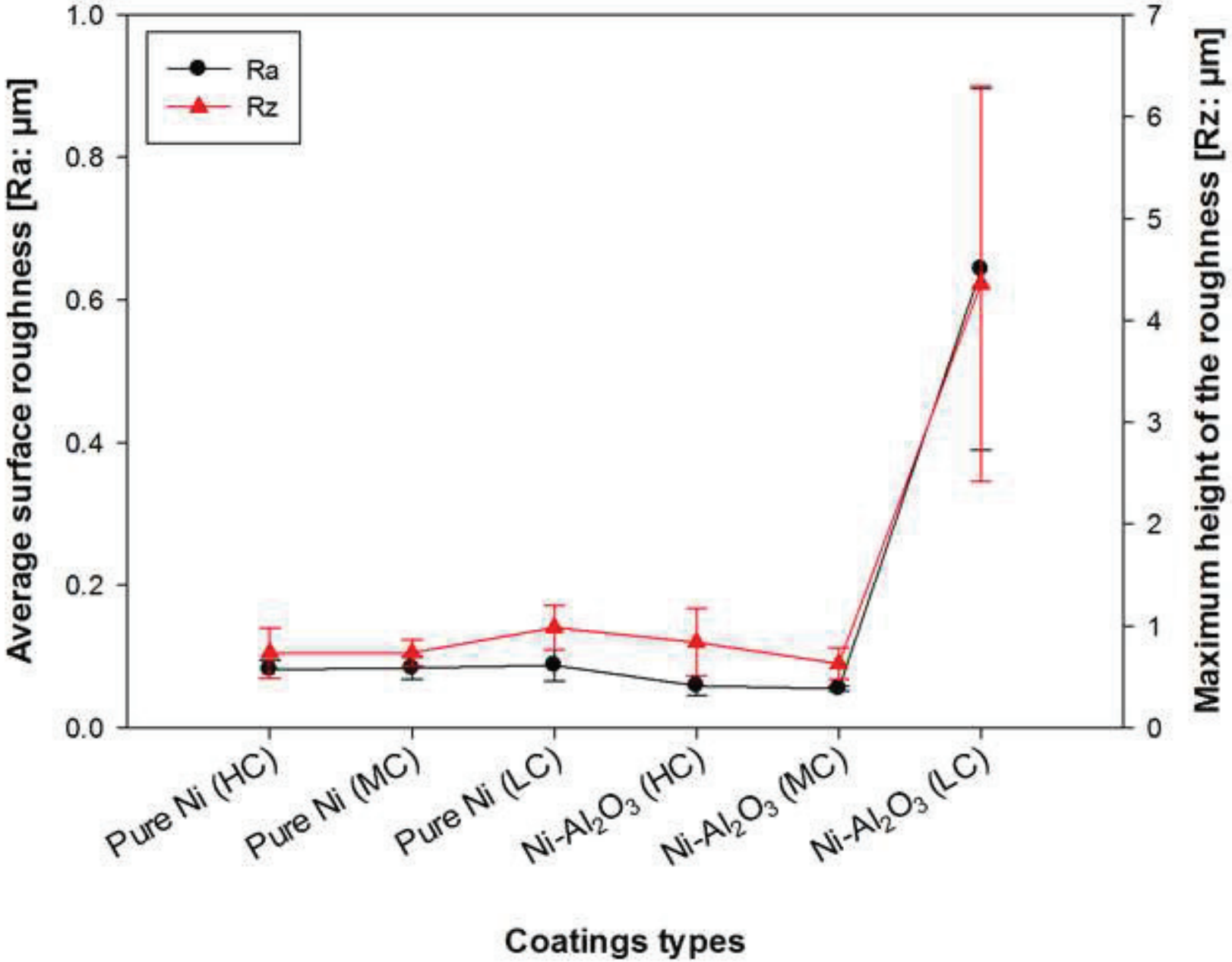

Figure3 Hardness and elastic modulus values of all coatings deposited from different bath concentration.

Click here to download Figure Figure3.tif

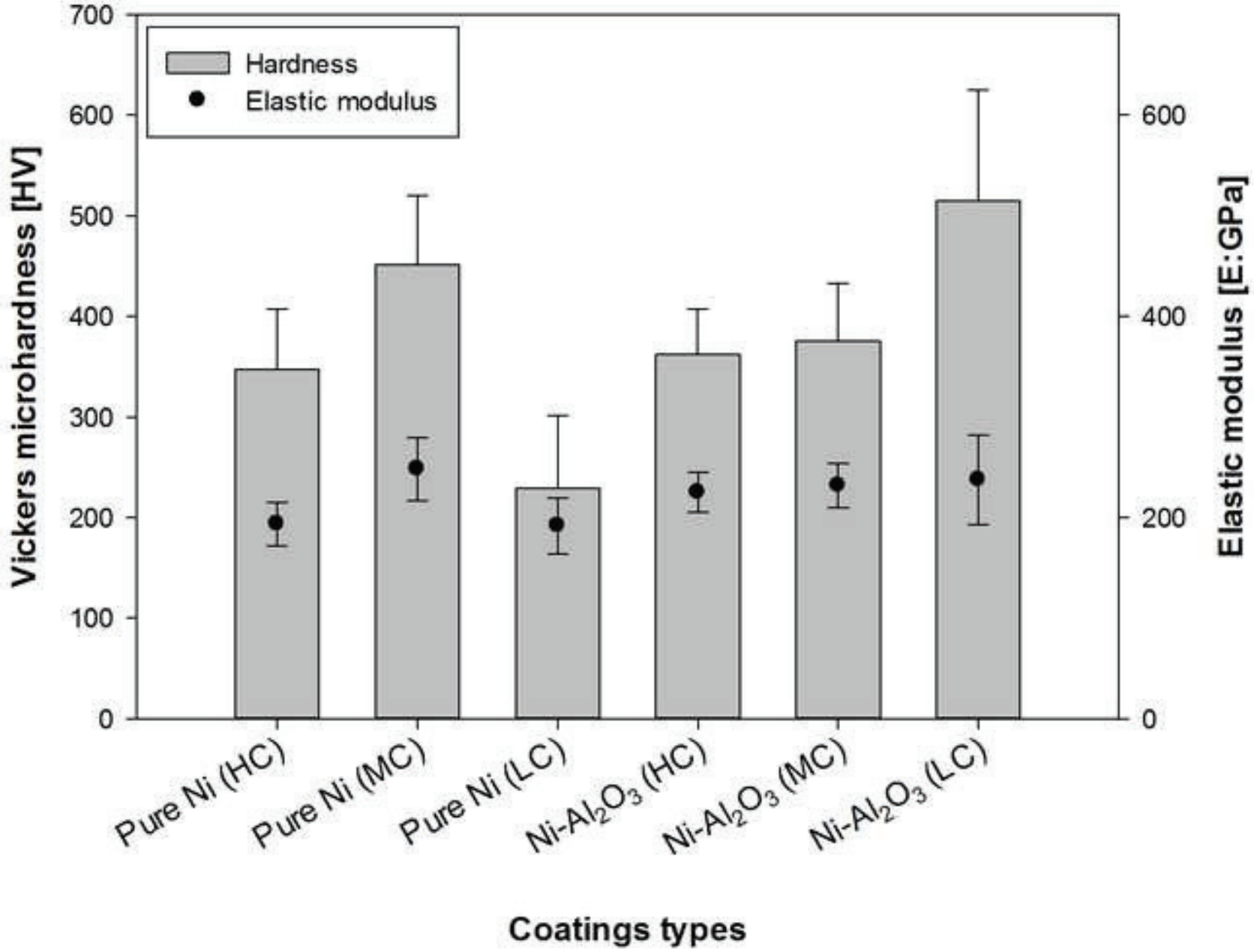

Figure4 Cross-sectional SEM images of pure nickel and nickel-based composite coatings electrodeposited with different electrolyte s

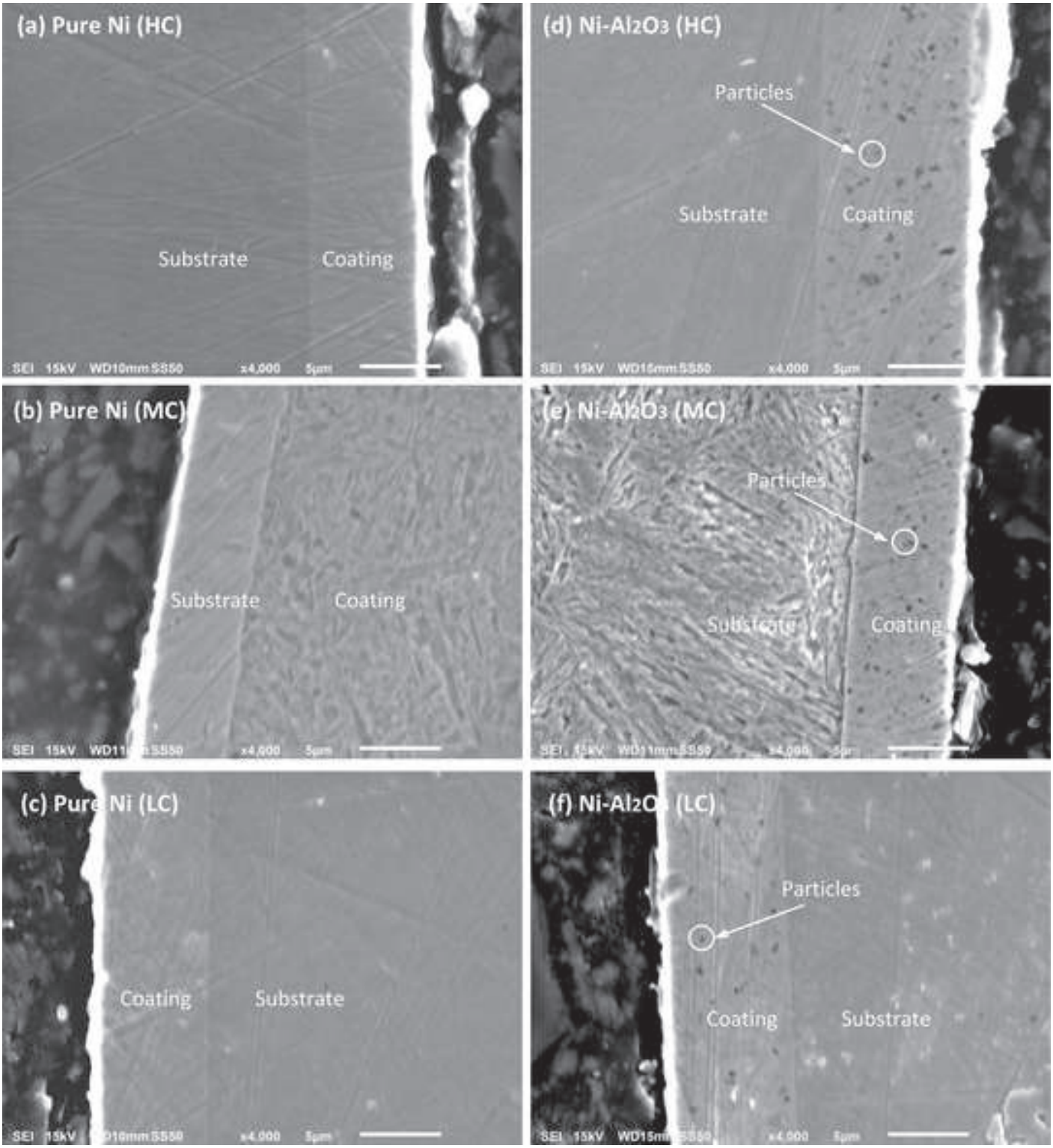

Figure5 The comparison of wear rates and mean-steady friction coefficient of pure nickel and nickel composite coatings electrodeposited with different current densities.



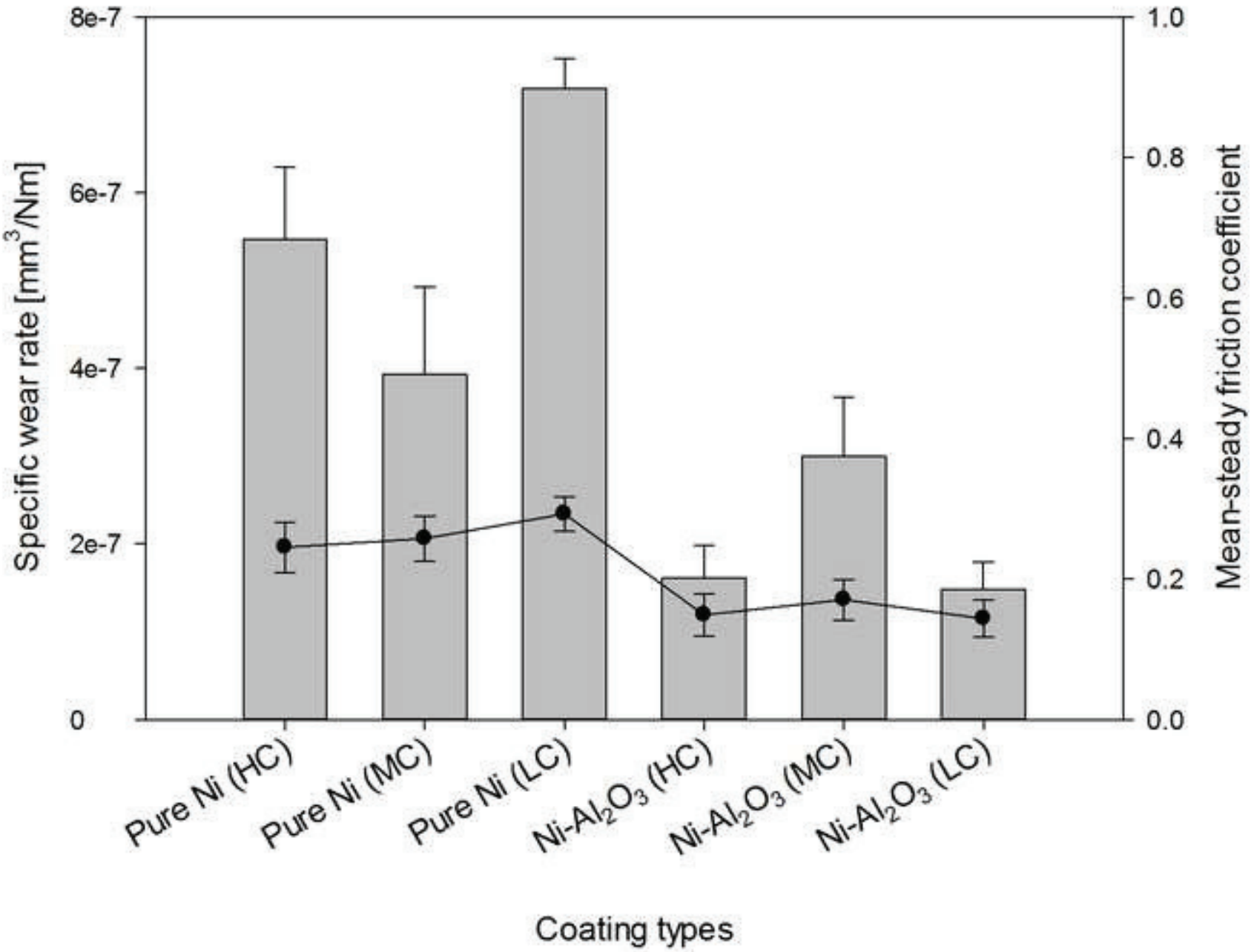

Figure6 The comparison of the surface energy and changing wettability behaviour of electrodeposited coatings with different electrolyte concentration

Click here to Download Figure Figure6.tif

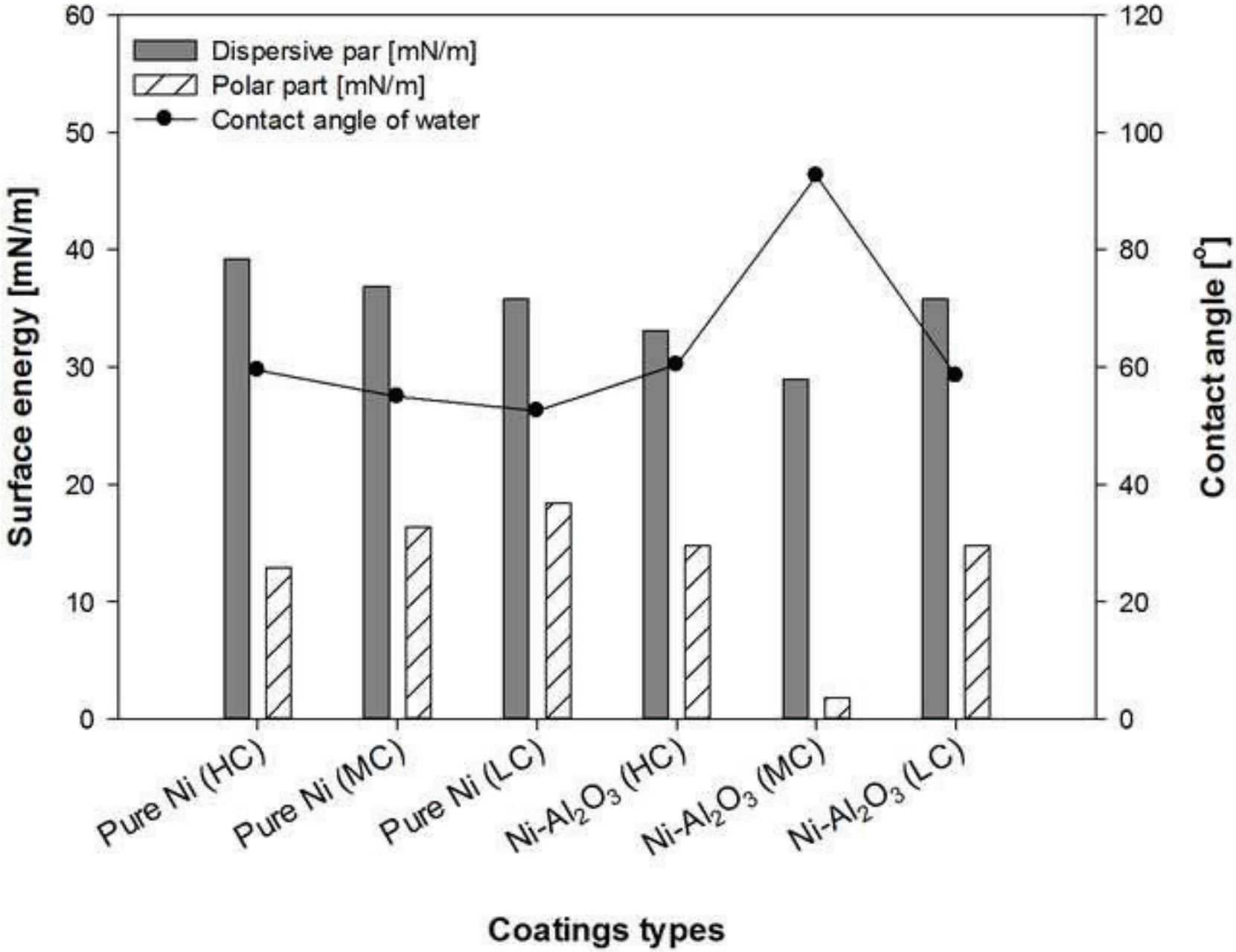

Figure7 Potentiodynamic polarization curves for electroplated coatings deposited with different electrolytic strength, in 3.5% NaCl solution. Click here to download Figure Figure7.tif

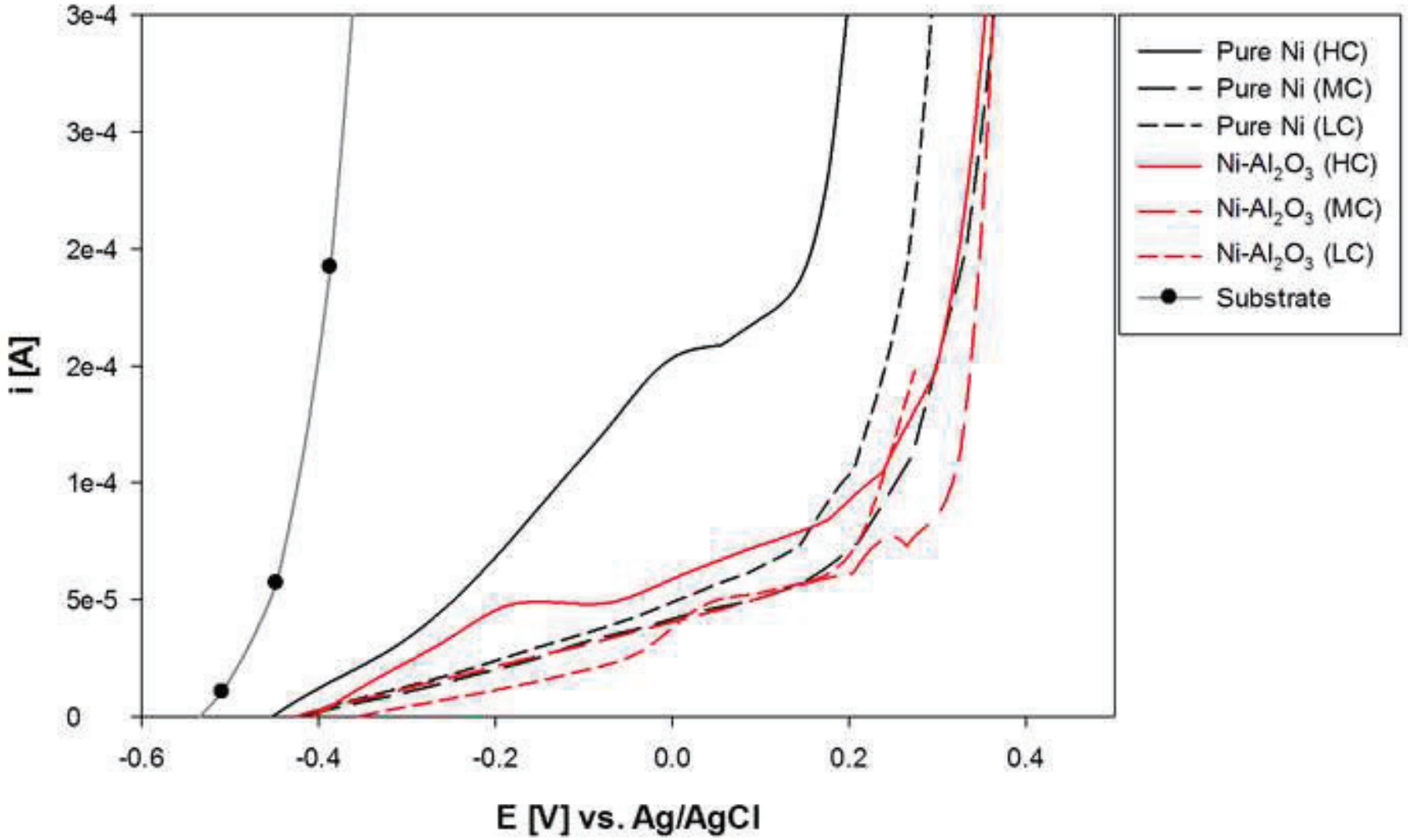

Figure8 Critical load values for electroplated coatings deposited with different electrolytic strength according to DIN EN 1071-3. Click here to download Figure Figure8.tif

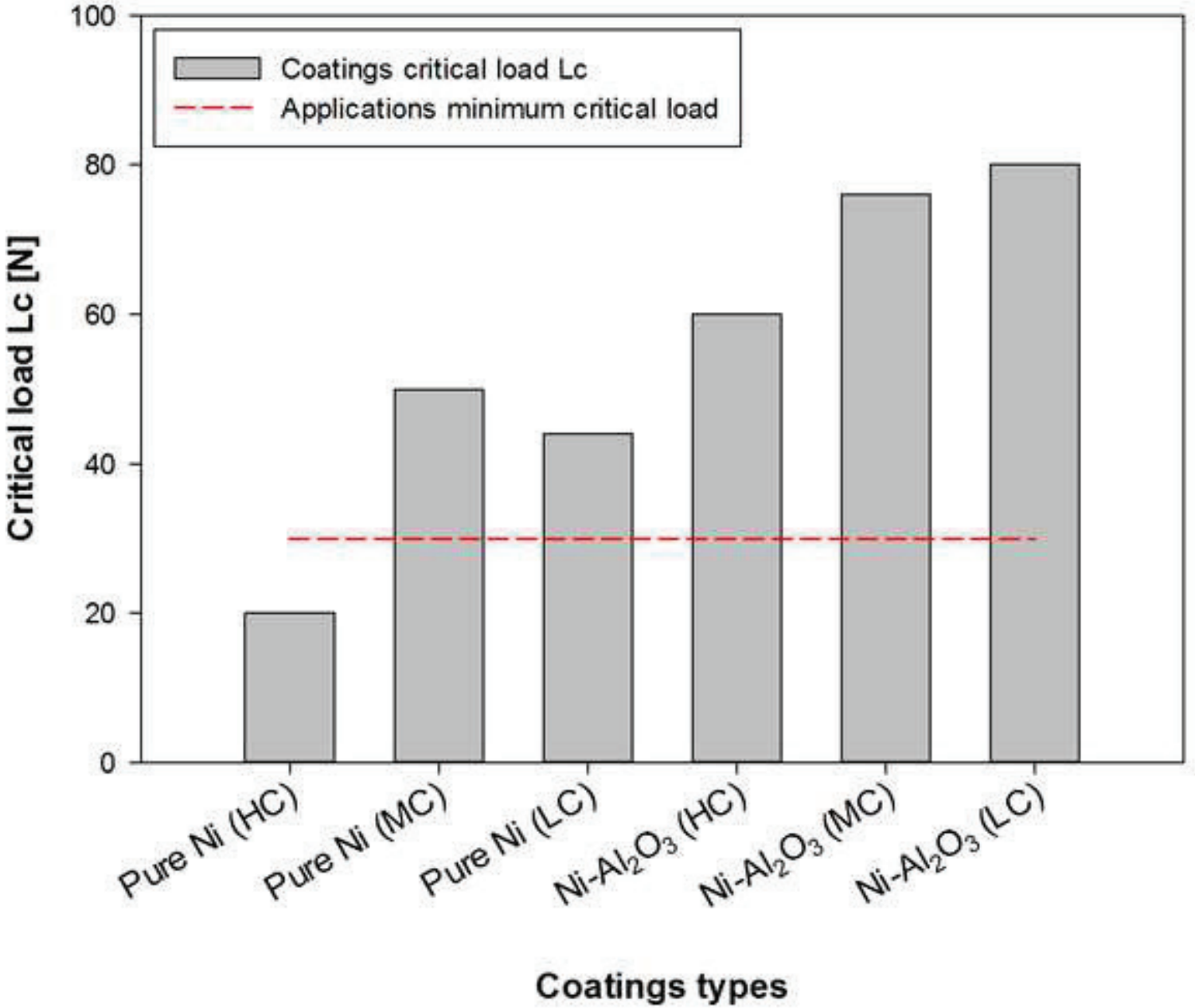

**Figure 1** Surface micrographs of pure nickel (a-c) and Ni-$Al_2O_3$ composite (e-g) coatings deposited through various bath concentrations (10kV, WD 11 and x2000).

**Figure 2** The variation in surface roughness parameters (Ra and Rz) of electrodeposited coatings with different electrolyte ionic strength.

**Figure 3** Hardness and elastic modulus values of all coatings deposited from different bath concentration.

**Figure 4** Cross-sectional SEM images of pure nickel and nickel-based composite coatings electrodeposited with different electrolyte ionic strength.

**Figure 5** The comparison of wear rates and mean-steady friction coefficient of pure nickel and nickel composite coatings electrodeposited with different electrolyte ionic strength.

**Figure 6** The comparison of the surface energy and changing wettability behaviour of electrodeposited coatings with different electrolyte ionic strength.

**Figure 7** Potentiodynamic polarization curves for electroplated coatings deposited with different electrolytic strength, in 3.5% NaCl solution.

**Figure 8** Critical load values for electroplated coatings deposited with different electrolytic strength according to DIN EN 1071-3.